Progress In Electromagnetics Research M, Vol. 98, 21–34, 2020

Comparison of High Impedance Textured Substrates for Suppression of Surface Waves in Microstrip Antennas with Solid and Hollow Metallic Pins

Manidipa Roy[1, *] and Ashok Mittal[2]

Abstract—High Impedance Textured Substrate is presented for suppression of Surface Waves in Microstrip Antennas. Surface wave propagation limits the radiation efficiency, bandwidth, gain, alters the main beam radiation pattern, and increases side lobe levels as well as the back lobes. A novel technique to suppress the surface waves with periodic arrangement of metallic cylindrical pins embedded in the substrate except the area underneath the radiating microstrip patch is presented here. Two structures with solid as well as hollow cylindrical pins are analysed with Spectral Domain Analysis. The textured pin bed structure creates negative permittivity and high capacitive impedance and thus suppresses the propagation of TM-surface waves. The gain of 11.83 dB with an enhancement of 6 dB over normal microstrip patch antenna is achieved. Further an increase of 1.61 dB gain with 12.27% improvement in radiation bandwidth is observed in the antenna structure with hollow cylindrical pins as compared to that of solid cylindrical pins. A uniform gain of more than 11 dB is achieved with a percentage bandwidth of 17.43%.

1. INTRODUCTION

Planar Microstrip antennas are used in most of the Microwave and Millimeter wave systems. They have many advantages such as low profile, light weight, conformal design, low cost of production, and robust nature. Microstrip Antennas are compatible with microwave monolithic integrated circuits and optoelectronic integrated circuits. Due to the merits, they have been utilized in most of the applications of mobile radio, satellite communications, radars, remote sensing, missiles, medicine, and many others.

Besides the obvious advantages, they have disadvantages such as low gain, narrow bandwidth, and poor radiation efficiency. Microstrip Antennas suffer with surface wave propagation beneath the radiation patch and in the dielectric. This leads to power loss and low radiation efficiency. The magnitude of these undesired waves depends on the substrate thickness, dielectric constant, and angles of reflection at the substrate metallic boundaries.

These surface waves (see Figure 1) are generated slightly downwards entering the substrate with a specific angle θ ranging from

$$\frac{\pi}{2} \leq \theta \leq \pi - \sin^{-1}\left(\frac{1}{\sqrt{\varepsilon_r}}\right) \tag{1}$$

These surface waves travel through the substrate and finally radiates through the edges, thus causing a reduction in gain, an increase in cross-polar levels, and increase of the cross coupling between array elements. The excitation of surface waves is a significant part of the total radiation energy [1–3]. Reducing the excitation of surface waves and their diffraction from edges will increase the radiation

Received 19 August 2020, Accepted 14 October 2020, Scheduled 27 October 2020
* Corresponding author: Manidipa Roy (manidipa4488@gmail.com).
[1] USICT, GGSIPU, Delhi, India. [2] Department of Electronics and Communication Engineering, AIACT&R, Delhi, India.

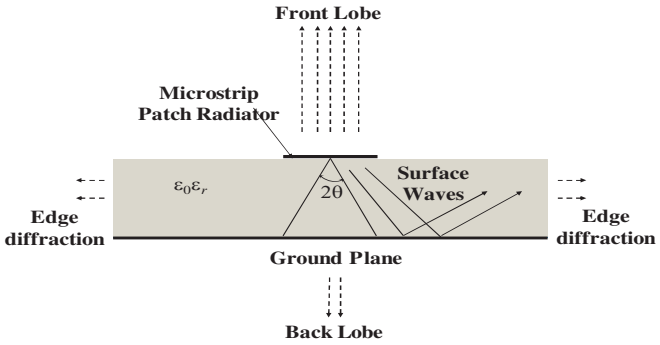

Figure 1. Schematic of waves in microstrip antennas.

efficiency and result in reduction in back radiation. Suppression of surface waves will save considerable amount of power loss and improve antenna performance and effects on radiation parameters like gain, bandwidth, and radiated power. Suppression of surface-waves will also decrease coupling in between antenna elements in an array, thus resulting in increase in gain and radiation efficiency.

Various techniques have been proposed in past for surface wave suppression in microstrip antennas [4–12]. Cylindrical pins embedded throughout the substrate has been presented for synthesis of Surface Reactance using an Artificial Dielectric by King et al. [6]. The electromagnetic bandgap is generated for surface wave propagation which leads to its suppression. Textured substrate has been used with metallic pins embedded in the dielectric throughout the substrate. The introduction of a triple layered dielectric substrate with the bottom most layer with an embedded pin bed structure was presented in [16].

In the proposed design, further improvements in gain and radiation efficiency have been achieved by designing a single layered textured pin dielectric substrate with hollow metallic pins. The results obtained with solid metallic pins (see Figure 2) are compared with that of hollow metallic pins and are reported here. In the present work, detailed designs and Spectral Domain Analysis are presented for a simple square microstrip patch antenna with a textured pin substrate, except beneath the radiating patch. Analysis has been carried out for solid cylindrical metallic pins and hollow cylindrical metallic pins (see Figure 3) embedded in the dielectric as textured substrate. The hollow metallic pins reduce the

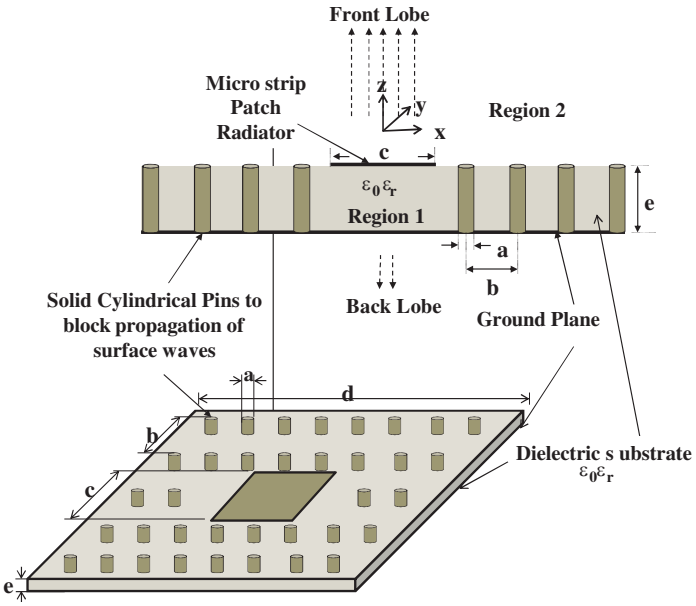

Figure 2. Pin substrate with solid metallic cylindrical pins.

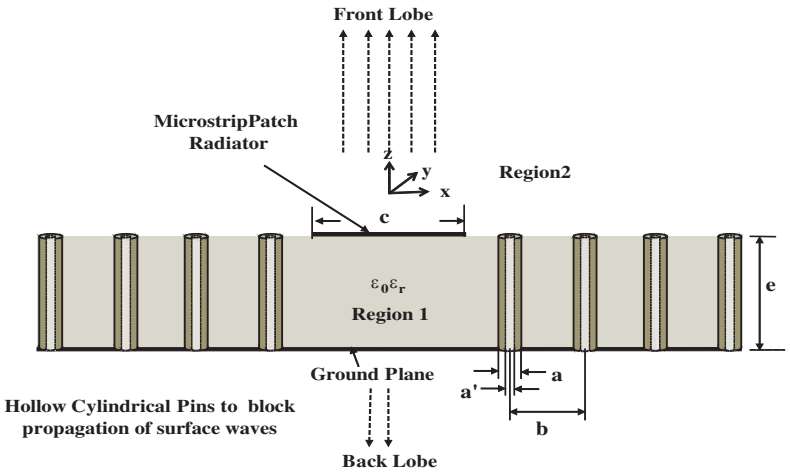

Figure 3. Pin substrate with hollow cylindrical pins.

conductor losses and thereby improve the gain and radiated power. A comparison of the performance of the two in terms of surface impedance, reflection coefficient, effective permittivity, and radiated power is presented. Simulations of the two structures are also done using Ansoft HFSSv12. The measurement results are in consonance with simulated and theoretical analysis and reveal the improvement in gain, radiated power, and bandwidth.

The design and analysis of the antenna structures has been done using Genetic Algorithm. Surface wave suppression in the planar antennas depends on multiple parameters. The initial step in this algorithm is to design the textured pin substrate with array of cylindrical metallic pins. The lattice spacing and diameter of pins is illustrated in Sections 2.1–2.2. The parametric analysis of the design parameters for the antenna designs is done next and shown in Section 2.3. After designing the antenna structures, the analysis of electromagnetic field components is done and postulated in Sections 3.1–3.4. The effect of embedding hollow metallic pins and its merits over solid metallic pins is also focused upon. Finally, the simulated and measured results are illustrated which validate the theoretical analysis. This is shown in Section 4.

2. DESIGN OF TEXTURED PIN ARTIFICIAL DIELECTRIC SUBSTRATE

The design methodologies and analysis of proposed antenna designs are explained in this section.

2.1. Solid Metallic Cylindrical Pins

The metallic cylinders, in the form of vias printed using PTH (Printed Through Hole) technique mounted on the ground plane, are designed as the texture on the substrate except under the radiating patch antenna (see Figure 2).

The high capacitive impedance offered by the textured pin substrate prohibits the propagation of TM-surface waves, which are transverse to the direction of antenna plane. The array of cylindrical metallic pins embedded in the dielectric substrate except under the patch preserves the radiation field inside the patch cavity and changes the effective permittivity and reflection coefficient. The artificial dielectric substrate specifically has to be designed with unity reflection coefficient, negative permittivity, and high capacitive impedance, as required for TM-Surface wave suppression.

An array of cylindrical metallic pins with radius 'a' and inter-element spacing 'b' is embedded in a dielectric substrate with relative permittivity $\varepsilon_h (= \varepsilon_d) = 4.4$. The height of the embedded pins is that of the substrate, i.e., 'e' = 1.6 mm. Design parameters of the array of metallic pins are calculated on the basis of refractive index. The effective spatial refractive index [6] of such an artificial dielectric medium is

$$\eta_{zy} = \left(\varepsilon_z \mu_y / \varepsilon_d \mu_d\right)^{1/2} \tag{2}$$

where ε_z = relative permittivity in z-direction, μ_y = relative permeability in y-direction, and ε_d and μ_d are the relative permittivity and relative permeability of the dielectric medium (host medium).

The wave propagates only if the refractive index η_{zy} is real, i.e.,

$$-1 < \cos(\eta_{zy}\theta) < 1 \tag{3}$$

where $\theta = k_d b$ is the electrical spacing and k_d the wave number in the artificial dielectric medium which defines the passbands. The value of refractive index $\eta_{zy}\theta$ is designed in a way that it satisfies the condition given in Eq. (3).

The basic methodology used for design of the EBG artificial dielectric substrate is to design the substrate with band gap or stopband characteristics for the propagation of TM_0 surface wave modes.

The refractive index of the artificial dielectric substrate is dependent on design parameters of the array of metallic cylindrical pins like pin diameter 'a' and lattice spacing 'b'. The dependence is shown as below [6]

$$\cos(\eta_{zy}\theta) = \cos\theta + A/\theta \sin\theta \tag{4}$$

$$A = \frac{\pi a}{(b \ln(b/\pi))}. \tag{5}$$

Here ε_d and μ_d are the dielectric constant and relative permeability, respectively. This theory is only valid if

$$a \ll b \ll \lambda_d/2 \tag{6}$$

where λ_d is the artificial dielectric medium wavelength.

The value of refractive index $\eta_{zy}\theta$ is designed in a way that it satisfies all the conditions given in Eqs. (3)–(6). The artificial dielectric medium is designed in such a manner that the propagation of waves through the substrate occurs only beyond the cut-off frequency of the medium which is kept above the resonant frequency of the patch antenna.

The radiation efficiency η [15] is defined by the ratio of the power radiated over the input power.

$$\eta = \frac{P_r}{P_t} = \frac{P_r}{P_r + P_I} \tag{7}$$

where P_r is the radiated power, P_t the total input power, and P_L the surface wave power loss. Analysis is presented in the following Section 3.3 for the radiated power.

The design parameters for solid cylindrical pins are as tabulated in Table 1. Parametric Analysis for optimization of radiation efficiency optimization is carried out by varying the pin diameter 'a' and array spacing 'b'.

Table 1. Design parameters solid metallic pins.

Parameter	'a'	'b'	'c'	'd'	'e'
Dimension (mm)	1	5	14	30	1.6

2.2. Hollow Metallic Cylindrical Pins

The textured pin substrate with hollow metallic pins is designed as shown in Figure 3. The design parameters are same as those kept for solid cylindrical pins as tabulated in Table 1. The hollow cylindrical pins with the same outer diameter considered for analysis are fabricated using PTH Technology. The inner diameter 'a'' (= 0.9 mm) is selected by the optimisation of radiation efficiency done using parametric analysis.

2.3. Parametric Analysis

Parametric Analysis for optimization of radiation efficiency is carried out by varying the lattice dimensions for the best performance. The radiation efficiency optimization is done by varying the

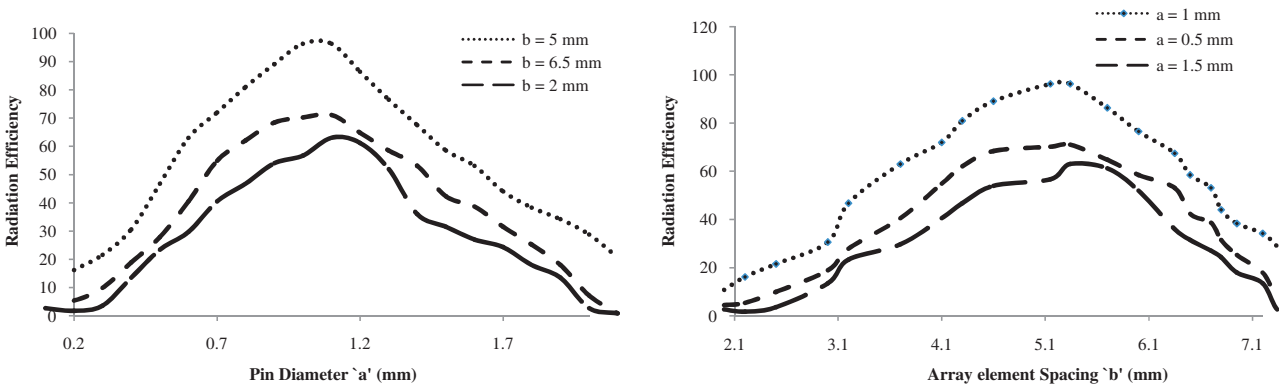

Figure 4. (a) Radiation efficiency with varying the pin diameter 'a'. (b) Radiation efficiency with varying the pin spacing 'b'.

two parameters, pin diameter 'a' and array spacing 'b'. The optimum value of pin diameter comes out to be 1 mm by varying the array spacing from 2 to 6.5 mm. The optimum value of array spacing comes out to be 5 mm by varying pin diameter from 0.5 mm to 1.5 mm (see Figures 4(a) and (b)).

The parametric study of the cylindrical thickness was done by varying the inner radius 'a' for the hollow cylindrical pins keeping all the other parameters of the solid cylindrical pin structure. It has been observed from Eqs. (22)–(28) that the radiated power, effective dielectric constant, and gain are dependent on cylindrical pin dimension. Simulation results as shown in Table 2 explain the effect of variation in gain due to change in dimensions of hollow cylindrical pins. The gain increases with increase in cylindrical pin inner diameter 'a''.

Table 2. Variation in cylindrical pin dimension for hollow cylindrical pins.

Outer Diameter (a in mm)	**Inner Diameter (a' in mm)**	**Resonant Frequency (GHz)**	**S_{11} (dB)**	**Gain (dB)**
1.0	0.3	7.74	−15.15	10.73
1.0	0.5	7.87	−16.54	11.32
1.0	0.7	7.91	−16.65	11.78
1.0	0.8	7.93	−16.95	11.81
1.0	0.9	7.94	−17.07	11.83

3. ANALYSIS OF TEXTURED PIN ARTIFICIAL DIELECTRIC SUBSTRATE

3.1. Spectral Domain Full Wave Analysis

The Spectral Domain Analysis has been done to compute the electric field components, radiation resistance, power radiated, effective dielectric constant, S_{11}, and surface impedance values of the microstrip patch antenna embedded on artificial dielectric with solid and hollow metallic pins, respectively.

For Electric Field Components, the x-directed current $\tilde{J}_x$ components in spectral domain are [1, 2]

$$\widetilde{E}_x\left(k_x, k_y, e\right) = \frac{-j}{\omega\varepsilon_0}\left[\frac{k_x^2 k_1 k_2 \sin\left(k_1 e\right)}{\beta^2 T_m} + \frac{k_x^2 k_0^2 \sin\left(k_1 e\right)}{\beta^2 T_e}\right]\tilde{J}_x \tag{8}$$

$$\widetilde{E}_y\left(k_x, k_y, e\right) = \frac{-j}{\omega\varepsilon_0}\left[\frac{k_x k_y k_1 k_2 \sin\left(k_1 e\right)}{\beta^2 T_m} - \frac{k_x k_y k_0^2 \sin\left(k_1 e\right)}{\beta^2 T_e}\right]\tilde{J}_x \tag{9}$$

$$\widetilde{E}_z\left(k_x,k_y,e\right) = \frac{-j}{\omega\varepsilon_0}\left[\frac{k_x k_1 \sin\left(k_1 e\right)}{T_m}\right]\tilde{J}_x \tag{10}$$

For the y-directed current $\tilde{J}_y$ on the air-dielectric interface at $z = e$, the electric field components in spectral domain are

$$\widetilde{E}_y\left(k_x,k_y,e\right) = \frac{-j}{\omega\varepsilon_0}\left[\frac{k_y^2 k_1 k_2 \sin\left(k_1 e\right)}{\beta^2 T_m} + \frac{k_x^2 k_0^2 \sin\left(k_1 e\right)}{\beta^2 T_e}\right]\tilde{J}_y \tag{11}$$

$$\widetilde{E}_y\left(k_x,k_y,e\right) = \frac{-j}{\omega\varepsilon_0}\left[\frac{k_x k_y k_1 k_2 \sin\left(k_1 e\right)}{\beta^2 T_m} - \frac{k_x k_y k_0^2 \sin\left(k_1 e\right)}{\beta^2 T_e}\right]\tilde{J}_y \tag{12}$$

$$\widetilde{E}_z\left(k_x,k_y,e\right) = \frac{-j}{\omega\varepsilon_0}\left[\frac{k_y k_1 \sin\left(k_1 e\right)}{T_m}\right]\tilde{J}_y \tag{13}$$

where

$$T_m = \varepsilon_{zz} k_2 \cos\left(k_1 e\right) + j k_1 \sin\left(k_1 e\right)$$
$$T_e = k_1 \cos\left(k_1 e\right) + j k_2 \sin\left(k_1 e\right)$$

For Region 1, i.e., $(0 < z < e)$

$$k_1^2 = k_z^2 = \varepsilon_{zz} k_0^2 - \beta^2 \text{ and } \operatorname{Im}\left(k_1\right) < 0$$

For Region 2, i.e., $(z > e)$

$$k_2^2 = k_z^2 = k_0^2 - \beta^2 \text{ and } \operatorname{Im}\left(k_2\right) < 0 \text{ and } \beta^2 = k_x^2 + k_y^2$$

where $\tilde{E}$ denotes the double Fourier transform of E and is defined as,

$$\widetilde{E}_z\left(k_x,k_y,e\right) = \iint_{-\infty}^{\infty} E(x,y,z) e^{-jk_x x} e^{-jk_y y} dx dy. \tag{14}$$

ε_{zz} is the effective dielectric constant of artificial dielectric substrate with embedded PTH metallic pins.

In a microstrip patch antenna fed by a probe current, there are two types of currents: excitation current J_e of the probe, and the surface current and patch current on metallization. Both the currents give rise to fields. According to the boundary condition, the tangential component of electric field along the metallic patch surface is zero i.e.,

$$\hat{z} \times [E(\widetilde{J}_e) + E(\widetilde{J}_s)] = 0 \tag{15}$$

and

$$E(\widetilde{J}_s) = \iint \widetilde{J}_s \cdot \bar{\bar{G}}(x,y|x_0,y_0) dx_0 dy_0 \tag{16}$$

where $\bar{\bar{G}}(x,y|x_0,y_0)$ is the Dyadic Green's function

Now

$$\tilde{E}\left(\bar{J}_s\right) = Z_s \bar{J}_s \tag{17}$$
$$Z_{in} = V/I_s \tag{18}$$
$$Z_{in} = -\int_0^h E_z dz \tag{19}$$

where $h = e$ is the height of the substrate, and Z_s is the surface impedance.

The radiation resistance is

$$R_r = \operatorname{Re}[Z_{in}] \tag{20}$$

The radiation resistance [13] comes out to be

$$R = \varepsilon_{eff} \cdot Z_0^2/(120 \cdot I_2) \tag{21}$$

where

$$I_2 = (k_0 e)^2 \cdot \left[0.53 - 0.03795 \cdot \left(k_0 c/2\right)^2 - \frac{0.03553}{\varepsilon_{eff}}\right]$$

3.2. Effective Dielectric Constant of the Textured Pin Substrate

A textured surface formed by a cylindrical pins array behaves like an impedance surface. The effect of losses due to cylindrical pins is important when the cross-section of the metallic wires is small, because the electric current along cylindrical pin with small radius is very large. The effect of losses becomes significant. If σ is the electrical conductivity of metal, the relative permittivity [6] will be

$$\varepsilon_{metal} = 1 + \frac{\sigma}{j\omega\varepsilon_0} = 1 + \frac{2}{j(\beta\delta_{skin})^2} \tag{22}$$

where $\delta_{skin} \approx \sqrt{2/\mu_0\sigma\omega}$ is the skin depth of the metal and $\beta = \omega/c$.

The effective dielectric constant for the wire medium 11, 14 is

$$\varepsilon_{zz}\,(\omega,k_Z) = 1 + \frac{1}{\left(\dfrac{\varepsilon_h}{(\varepsilon_{metal} - \varepsilon_h)f_v} - \dfrac{(\beta_h^2 - k_Z^2)}{\beta_p^2}\right)} \tag{23}$$

where f_v is the volume fraction of the cylindrical pins; β_p and β_h are the phase constant (wave number) in plasma (artificial dielectric) and host medium respectively; and k_z is the z-component of the wave vector $k = (k_x,\, k_y,\, k_z)$ of the plane wave.

For solid cylindrical pins $f_v = \pi(\frac{a}{b})^2$, and the value of $\varepsilon_{zz}(\omega,k_Z)$ for textured pin substrate with solid metallic cylindrical pins is $-1.34 - j0.001$.

For hollow cylindrical pins $f_v = \frac{\pi(a-a')^2}{4b^2}$ is the volume fraction of the rods.

Here 'a' is the outer diameter of the hollow metallic rod, 'a'' the inner diameter of the hollow metallic rod, 'b' the lattice spacing, and the value of $\varepsilon_{zz}(\omega,k_Z)$ with hollow metallic cylindrical pins is $-1.92 - j0.001$. Compared to solid PTH pins, the hollow pins exhibit lesser values for ε_{zz}.

Thus the value of ε_{eff} is

$$\varepsilon_{eff} = \varepsilon_0\varepsilon_h(\hat{u}_x\hat{u}_x + \hat{u}_y\hat{u}_y + \varepsilon_{zz}(\omega,k_z)\hat{u}_z\hat{u}_z) \tag{24}$$

where ε_h is the relative permittivity of the medium with embedded cylindrical pins, $\beta_h = \beta\sqrt{\varepsilon_h}$ the wave number in the textured dielectric medium, $\beta = k = \omega/c$ the wave number in free space, and β_p the plasma wave number.

$$(\beta_p b)^2 = \frac{2\pi}{\ln\left(\dfrac{b}{2\pi a}\right) + 0.5275}. \tag{25}$$

The effective dielectric constant for antenna structures shows negative permittivity of the textured dielectric substrate.

3.3. Radiated Power and Radiation Efficiency

The power radiated is given by [13–15]

$$P_R = \frac{V_0^2 \cdot 60}{Z_0^2 \cdot \pi}\varepsilon_{eff}\int_0^{\pi/2}\int_0^{2\pi}\{L * (M+N)\}\sin\theta d\theta d\emptyset \tag{26}$$

where

$$L = \frac{\cos^2\left(\dfrac{\pi\sin\theta\cos\emptyset}{2\sqrt{\varepsilon_{eff}}}\right)\cdot \mathrm{sinc}^2(wk_0\sin\theta\sin\emptyset/2)}{\left(\sin^2\theta\cos^2\emptyset - \varepsilon_{eff}\right)^2}$$

$$M = \frac{\left(\cos^2\theta\sin^2\emptyset\right)}{\left(\varepsilon_r - \sin^2\theta\right)\cot^2\left(hk_0\sqrt{\varepsilon_r - \sin^2\theta}\right) + \cos^2\theta}$$

$$N = \frac{\cos^2\theta\cos^2\emptyset\left(\varepsilon_r - \sin^2\theta\right)}{\left(\varepsilon_r - \sin^2\theta\right) + \varepsilon_r^2\cos^2\theta\cot^2\left(hk_0\sqrt{\varepsilon_r - \sin^2\theta}\right)}$$

where V_0 is the voltage applied at $x = 0$, $w = c$ the width of the microstrip radiator, $h(= e)$ the substrate thickness, Z_0 the characteristic impedance, and k_0 the cutoff wave number.

The comparison of power radiated for same antenna embedded on three different dielectric substrates, i.e., simple dielectric, textured pin substrate with solid metallic pins, textured pin substrate with hollow metallic pins at design frequency 7.94 GHz, is given in Table 3.

Table 3. Comparison of radiated power.

Antenna Structure	Peak Radiated Power-Theoretical (dBm)	Peak Radiated Power-Simulation (dBm)
Antenna embedded on simple dielectric substrate	−45	−45
Antenna embedded on textured pin substrate with solid metallic pins	−31	−31
Antenna embedded on textured pin substrate with hollow metallic pins	−28	−28

The radiation efficiency η is defined by the ratio of the power radiated over the input power (refer Eq. (7)). Figure 5 shows the comparison of radiation efficiency of the microstrip patch antenna embedded on a simple dielectric substrate and microstrip antennas with proposed structure embedded with solid and hollow cylindrical metallic pins.

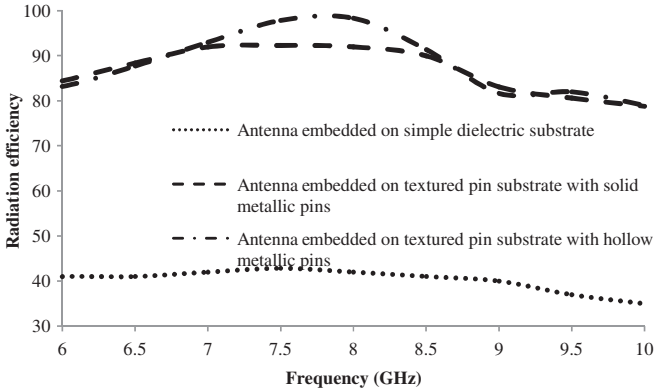

Figure 5. Comparison of the radiation efficiency.

3.4. Dispersion Characteristics

The dispersion characteristic of TM mode supported by the wire medium is [11]

$$\beta_h^2 = \beta_p^2 + k^2 \tag{27}$$

For the densely packed wires surface impedance, Z_s [6] is

$$Z_S = \frac{j\eta_0 \tan(\beta_h L)}{\sqrt{\varepsilon_h}} \tag{28}$$

where $\eta_0 = \sqrt{\mu_0/\varepsilon_0}$ is the free-space impedance. The textured surface is formed by a square lattice of metallic pins, embedded in a dielectric substrate with permittivity ε_h and height $L = e$.

TM-surface wave modes propagate when Z_s is inductive and are suppressed when Z_s is capacitive.

Variation of theoretically calculated Z_s with Frequency ranging from 6–9 GHz is plotted in Figure 6. Using Field Theory the theoretical value of S_{11} (dB) is calculated from reflection coefficient [11]

$$\rho = \frac{-\left(\beta_h\beta_p^2\tan\left(\beta_h L\right) - k_{||}^2\gamma_{TM}\tanh\left(\gamma_{TM}L\right) + \varepsilon_h\gamma_0\left(\beta^2 + k_{||}^2\right)\right)}{\left(\beta_h\beta_p^2\tan\left(\beta_h L\right) - k_{||}^2\gamma_{TM}\tanh(\gamma_{TM}L) - \varepsilon_h\gamma_0(\beta^2 + k_{||}^2)\right)} \tag{29}$$

where $\gamma_{TM} = \sqrt{\beta_p^2 + k_{||}^2 - \beta_h^2}$ and $k_{||} = (k_x, k_y, 0)$ is the component of the wave vector parallel to the interface (for a propagating wave $k_{||} = \beta\sin\theta$ with $\beta = \omega/c$ and θ, the angle of incidence), and $\gamma_0 = \sqrt{k_{||}^2 - \beta^2}$.

$$S_{11} = -20\log|\rho| \tag{30}$$

Variation of theoretically calculated S_{11} with frequency is plotted as shown in Figure 6.

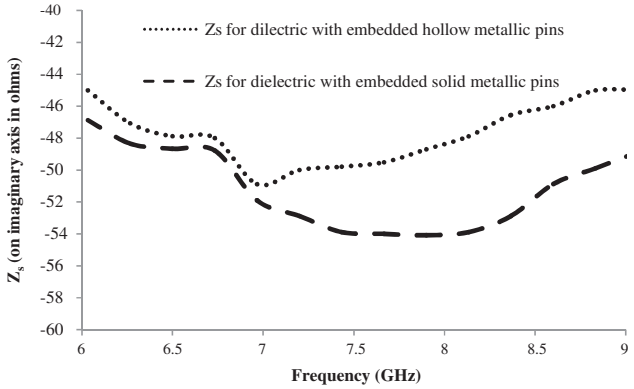

Figure 6. Variation of theoretically calculated Z_s with Frequency.

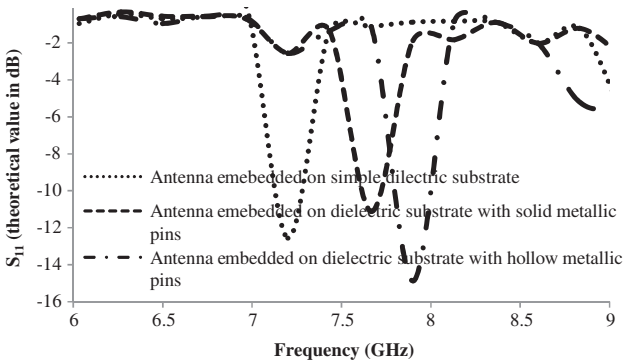

Figure 7. Variation of theoretically calculated S_{11} with frequency.

In Figure 7, a resonant frequency shift is observed when the antenna is designed on an artificial dielectric substrate. The effective dielectric constant gradually decreases when the antenna is designed on an artificial dielectric substrate with hollow metallic pins. The frequency shift is observed as the resonant frequency is increasing function with respect to decreasing effective permittivity of the substrate.

The antenna structure embedded on a dielectric substrate with hollow metallic pins is theoretically designed to suppress TM surface wave propagation. The suppression of surface wave propagation is validated from the results obtained for effective permittivity, surface impedance, and radiated power as tabulated in Table 4.

4. ANALYSIS OF THEORETICAL, SIMULATED AND EXPERIMENTAL RESULTS

The simple square patch antenna embedded on a dielectric substrate is designed at 7.25 GHz, and the gain is observed to be 6 dB. The same design is translated on a dielectric substrate with an embedded solid cylindrical pin bed structure. The gain of 10.51 dB is observed for resonance bandwidth centred at resonant frequency 7.6 GHz. For the same patch etched on a dielectric substrate embedded with hollow metallic pins, the gain improvement of 1.61 dB is observed as shown in Figure 8.

For the S_{11} characteristics of the antenna embedded on a textured pin substrate with hollow metallic pins, simulated results have been presented at design frequency of 7.94 GHz (see Figure 9(a)).

For the S_{11} characteristics of antenna embedded on a textured pin substrate with solid metallic pins, simulated results have been presented at the design frequency of 7.6 GHz (see Figure 9(b)).

The realized S_{11} characteristics show bandwidth improvement in the case of the antenna embedded on a dielectric substrate with hollow metallic pins. The realized percentage bandwidth in Figure 9(a) is 17.43%, and realized bandwidth in Figure 9(b) is 5.16%. The improvement in bandwidth of 12.27% is

Table 4. Significance of theoretically calculated parameters.

Parameters	Value	Significance
Antenna Design Parameters	Pin Diameter 'a', Pin Spacing 'b' and inner diameter 'a''	Diameters and Pin Spacing are calculated using parametric analysis so as to achieve maximum radiation efficiency
Permittivity	$-(1.92 + j0.001)$	Negative Permittivity is observed in artificial dielectric substrate, this enables suppression of surface waves
Surface Impedance	$-j50.08\,\Omega$	Capacitive surface impedance is observed which shows suppression of TM-surface wave modes, this is validated by enhancement in radiated power
Radiated Power	-28 dBm	Considerable increase in radiated power is observed in case of antenna embedded on textured pin substrate with hollow metallic pins

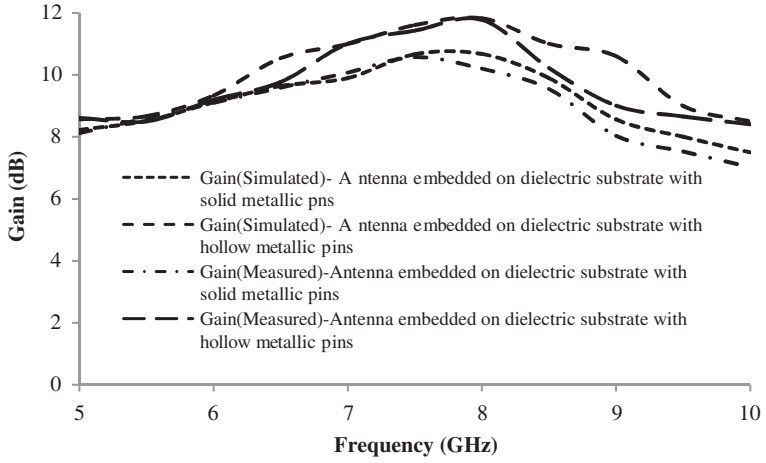

Figure 8. Gain characteristics of antenna embedded on textured pin substrate.

observed. This is due to the improvement in surface impedance as shown in Figure 5, and improvement in bandwidth is observed. The capacitive surface impedance is responsible for TM- surface wave suppression. This is responsible for the improvement in gain and bandwidth. The realized gain characteristics are plotted in Figure 8.

Fabricated prototypes of solid and hollow cylindrical pins textured substrates are shown in Figure 10. Radiation pattern shows considerable amount of increase in beamwidth of major lobe of the antenna embedded on a textured pin substrate with hollow metallic pins (at 7.94 GHz) as compared to the antenna embedded on solid metallic pins (at 7.6 GHz) on an FR4 dielectric substrate Figure 11 and Figure 12.

The near E field distributions for the antenna embedded on an artificial dielectric with hollow metallic pins and with solid metallic pins are presented in Figure 13. Comparisons of results are presented for the two antenna structures in Table 5. A considerable improvement in percentage bandwidth, gain, and HPBW is being observed.

Table 6 shows the comparison with antenna structures proposed earlier with similar objectives. It shows that the proposed antenna design with hollow metallic pins postulates superior gain characteristics of around 11.83 dB.

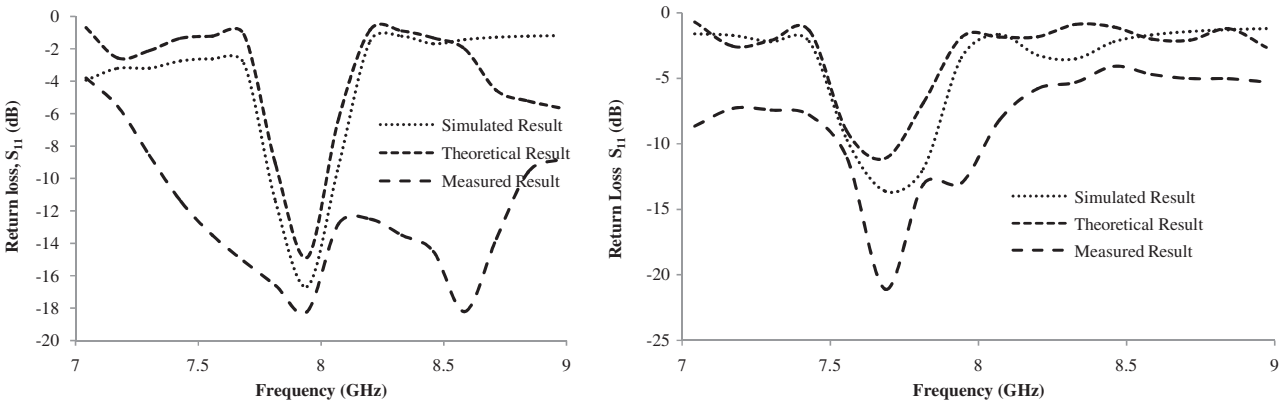

Figure 9. (a) S_{11} characteristics of antenna embedded on dielectric substrate with hollow metallic pins. (b) S_{11} characteristics of antenna embedded on dielectric substrate with solid metallic pins

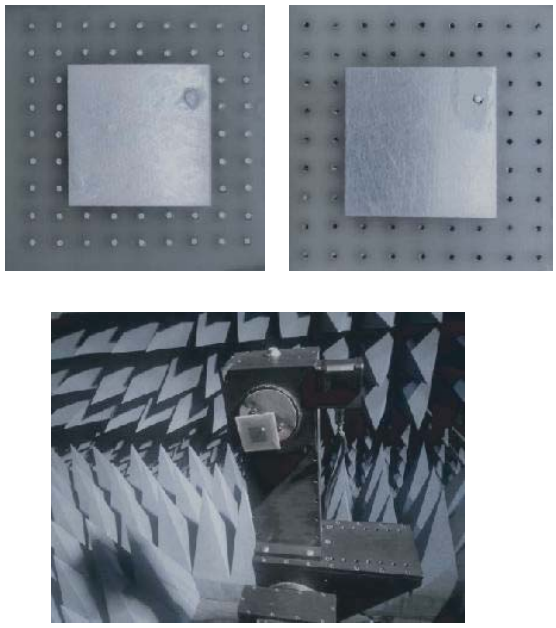

Figure 10. Fabricated prototypes of solid and hollow pin textured substrate and testing in anechoic chamber.

Table 5. Comparison of measured antenna parameters.

Antenna Design	Percentage Bandwidth	Gain (dB)	HPBW Cross-Polar (degrees)	HPBW Co-Polar (degrees)
Antenna embedded on dielectric substrate with solid metallic pins	5.16	10.23	54	74
Antenna embedded on dielectric substrate with hollow metallic pins	17.43	11.54	83	91

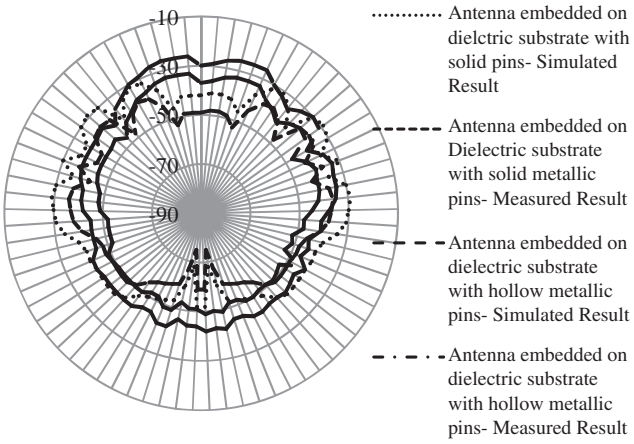

Figure 11. Radiation pattern of radiated power (dBm) vs. theta (degrees).

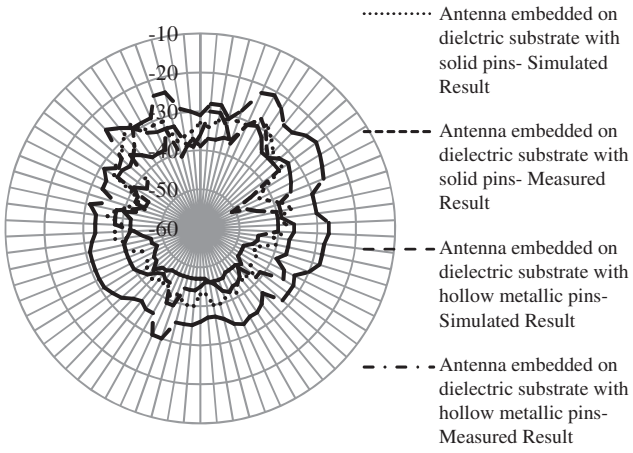

Figure 12. Radiation pattern of radiated power (dBm) vs. phi (degrees).

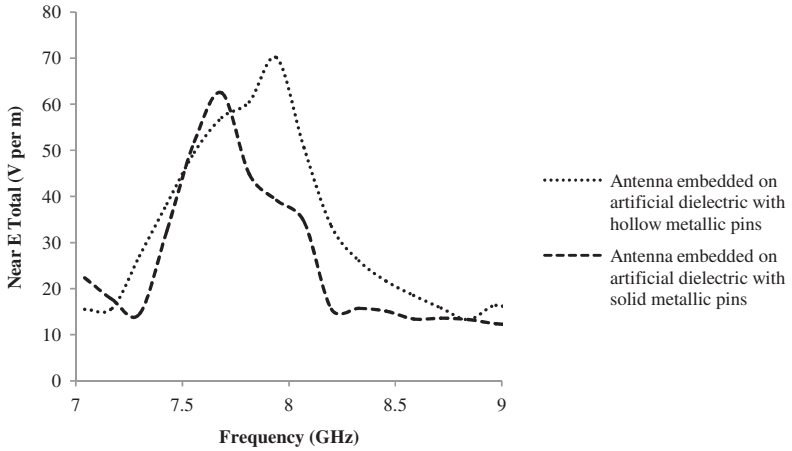

Figure 13. Near E field distributions for antenna embedded on artificial dielectric with hollow metallic pins and with solid metallic pins.

Table 6. Comparison of measured antenna parameters with the latest state of art references.

Reference No.	Year of Publication	Gain	Spacing between pins	Technique used for artificial dielectric design
[17]	2006	10.32 dBi	0.2 mm	Array of cylindrical pins with dielectric cover
[18]	2012	6.99 dB	1.5 mm	Surface Integrated artificial dielectric
[19]	2014	9.1 dBi	4.5 cm	Array of cylindrical hollow cylinders
[20]	2016	9.8 dB	18 mm	Array of mushroom like EBG with pair of slots on top dielectric

5. CONCLUSION

Surface wave propagation in microstrip antennas and arrays limits the radiation efficiency, bandwidth, and gain. To suppress the surface waves, a technique with periodic arrangement of metallic cylindrical pins embedded in a substrate except the area underneath the radiating microstrip patch has been presented. Two structures with solid as well as hollow cylindrical pins have been analysed. The designed dielectric substrate offers negative permittivity and very high capacitive impedance for TM surface wave suppression. The solid cylindrical pins suffer from problem of conductor loss. This problem is solved to a great extent by using hollow metallic pins. The hollow metallic pins show an improvement in radiated power and gain, and the results are validated through simulation, measurement, and theoretical analysis. The reason behind this observation is the reduction in conductor loss due to the presence of less conducting material in the metallic pin. The effect of variation of sleeve dimension has also been presented. The analysis presents good consonance between the theoretical, simulated and experimental results. The proposed antenna using a textured pin substrate with hollow metallic pins exhibits improved radiation characteristics.

REFERENCES

1. Garg, R. and P. Bhartia, *Microstrip Antenna Design Handbook*, 43–48, Artech House, London, 2001.
2. James, J. R. and P. S. Hall, *Handbook of Microstrip Antenna*, 116–118, Peter Peregrinus, London, 1989.
3. Emhemmed, A. S. and A. A. Aburwein, "Surface waves reduction in microstrip antennas," *Proc. 5th IEEE International Symposium on Microwave, Antenna, Propagation and EMC Technologies for Wireless Communications*, 438–442, Chengdu, China, 2013.
4. Brown, J. M. A., "Artificial dielectrics having refractive indices less than unity," *Proc. IEE, Radio Section, Monograph*, Vol. 62, 11–23, 1953.
5. Rotman, W., "Plasma simulation by artificial dielectrics and parallel plate media," *IRE Transactions on Antennas and Propagation*, 81–96, January 1961.
6. King, R. J., D. V. Thiel, and K. S. Park, "The synthesis of surface reactance using an artificial dielectric," *IEEE Transactions on Antennas and propagation*, Vol. 31, No. 3, 471–476, May 1983.
7. Seivenpiper, D. and B. Zhang, "High impedance electromagnetic surfaces with a forbidden frequency band," *IEEE Transactions on Antennas and Propagation*, Vol. 47, No. 11, 2059–2074, November 1999.
8. Engheta, N., "An idea for thin subwavelength cavity resonators using metamaterials with negative permittivity and permeability," *IEEE Transactions on Antennas and Propagation*, Vol. 1, 10–13, October 2002.
9. Fallah-Rad, M. and L. Shafai, "Gain enhancement in linear and circularly polarised microstrip patches antennas using shorted metallic patches," *IEE Proceedings — Microwaves, Antennas and Propagation*, Vol. 152, No. 3, 138–148, June 2005.
10. Buell, K., H. Mosallaei, and K. Sarabandi, "Electromagnetic metamaterial insulator to eliminate substrate surface waves," *Proc. of IEEE Antennas and Propagation Society International Symposium*, 574–577, 2005.
11. Silveirinha, M., G. Carlos A. Fernandes, and J. R. Costa, "Electromagnetic characterization of textured surfaces using textured pins," *IEEE Transactions on Antennas and Propagation*, Vol. 56, No. 2, 405–415, February 2008.
12. Komanduri, V. R., D. R. Jackson, J. T. Williams, and A. R. Mehrotra, "A general method for designing reduced surface wave microstrip antennas," *IEEE Transactions on Antennas and Propagation*, Vol. 61, No. 6, 2887–2894, June 2013.
13. Gera, A. E., "The radiation resistance of a microstrip element," *IEEE Transactions on Antennas and Propagation*, Vol. 38, No. 4, 568–570, April 1990.

14. Silveirinha, M. G., "Nonlocal homogenization model for a periodic array of ε-negative rods," *Phys. Rev. E*, Vol. 73, No. 4, 046612 1-10, April 2006.
15. Pozar, D. M., "Rigorous closed form expressions for the surface wave loss of printed antennas," *Electronic Letters*, Vol. 26, No. 13, 954–956, June 1990.
16. Roy, M. and A. Mittal, "Surface wave suppression in LHCP microstrip patch antenna embedded on textured pin substrate," *Progress In Electromagnetic Research C*, Vol. 89, 171–180, 2019.
17. Qu, D., L. Shafai, and A. Foroozesh, "Improving microstrip patch antenna performance using EBG substrates," *IEE Proceedings — Microwaves, Antennas and Propagation*, Vol. 153, No. 6, 558–563, December 2006.
18. Ghosh, A., B. Sarkar, and A. De, "High gain compact rectangular microstrip patch antenna using substrate integrated artificial," *2012 International Conference on Communications, Devices and Intelligent Systems (CODIS)*, 224–227, Kolkata, 2012.
19. Mukherjee, B., et al., "A novel hemispherical dielectric resonator antenna on an electromagnetic band gap substrate for broadband and high gain systems," *Int. J. Electron. Commun. (AEÜ)*, Vol. 68, No. 12, 1185–1190, 2014.
20. Han, Z.-J., W. Song, W.-J. Li, and X.-Q. Sheng, "High-gain and low-profile EBG patch antenna design," *2016 Progress in Electromagnetic Research Symposium (PIERS)*, 1676–1679, Shanghai, China, 2016.